EVIDENCE FOR GAMMA-RAY EMISSION FROM THE LOW-MASS X-RAY BINARY SYSTEM FIRST J102347.6+003841

P. H. T. TAM[1], C. Y. HUI[2], R. H. H. HUANG[1], A. K. H. KONG[1,8], J. TAKATA[3], L. C. C. LIN[4], Y. J. YANG[5], K. S. CHENG[3],
AND R. E. TAAM[6,7]

[1] Institute of Astronomy and Department of Physics, National Tsing Hua University, Hsinchu, Taiwan; phtam@phys.nthu.edu.tw
[2] Department of Astronomy and Space Science, Chungnam National University, Daejeon, Republic of Korea
[3] Department of Physics, University of Hong Kong, Pokfulam Road, Hong Kong
[4] Graduate Institute of Astronomy, National Central University, Jhongli, Taiwan
[5] Astronomical Institute "Anton Pannekoek," University of Amsterdam, Amsterdam, The Netherlands
[6] Department of Physics and Astronomy, Northwestern University, 2131 Tech Drive, Evanston, IL 60208, USA
[7] Academia Sinica Institute of Astronomy and Astrophysics–TIARA, Taipei, Taiwan

ABSTRACT

The low-mass X-ray binary (LMXB) system FIRST J102347.6+003841 hosts a newly born millisecond pulsar (MSP) PSR J1023+0038 that was revealed as the first and only known rotation-powered MSP in a quiescent LMXB. While the system is shown to have an accretion disk before 2002, it remains unclear how the accretion disk has been removed in order to reveal the radio pulsation in 2007. In this Letter, we report the discovery of γ-rays spatially consistent with FIRST J102347.6+003841, at a significance of seven standard deviations, using data obtained by the *Fermi Gamma-ray Space Telescope*. The γ-ray spectrum can be described by a power law (PL) with a photon index of 2.9 ± 0.2, resulting in an energy flux above 200 MeV of $(5.5 \pm 0.9) \times 10^{-12}$ erg cm^{-2} s^{-1}. The γ-rays likely originate from the MSP PSR J1023+0038, but also possibly from an intrabinary shock between the pulsar and its companion star. To complement the γ-ray study, we also re-investigate the *XMM-Newton* data taken in 2004 and 2008. Our X-ray spectral analysis suggests that a broken PL with two distinct photon indices describes the X-ray data significantly better than a single PL. This indicates that there exists two components and that both components appear to vary with the orbital phase. The evidence for γ-ray emission conforms with a recent suggestion that γ-rays from PSR J1023+0038 may be responsible for ejecting the disk material out of the system.

Key words: gamma rays: stars – pulsars: individual (PSR 1023+0038) – X-rays: binaries

1. INTRODUCTION

Radio millisecond pulsars (MSPs) are rotating neutron stars (NSs) that have been spun up via the transfer of angular momentum through accretion in low-mass X-ray binary (LMXB) systems (Bhattacharya & van den Heuvel 1991). Recently, a total of nine γ-ray emitting MSPs have been identified through their γ-ray pulsations (Abdo et al. 2009a, 2010a).

Theoretical models have long suggested that an accretion-powered MSP in an LMXB will turn on as a rotation-powered MSP when the system is in quiescence (Alpar et al. 1982). How exactly the transition happens is not completely understood; however, it is widely believed that radio MSPs can only turn on after the accretion disk is removed. Suggested mechanisms include the pulsar wind ablation (Wang et al. 2009), heating associated with the deposition of γ-rays from the MSP (Takata et al. 2010a), and the propeller effect (Romanova et al. 2009).

PSR J1023+0038 is the first and only known rotation-powered MSP in a quiescent LMXB, namely, FIRST J102347.67+003841.2 (hereafter J1023). J1023 was identified as an LMXB in 2006 (Homer et al. 2006) and the radio MSP was found subsequently (Archibald et al. 2009). The source clearly showed an accretion disk before 2002 (Wang et al. 2009) and the disk has since disappeared (Archibald et al. 2009); radio pulsation was found in 2007 (Archibald et al. 2009). Therefore, PSR J1023+0038 is considered as a newly born MSP, representing the long sought-after missing link of a rotation-powered MSP descended from an LMXB.

The spin-down power of PSR J1023+0038 ($L_{sd} \leqslant 3 \times 10^{35}$ erg s^{-1}; Archibald et al. 2009) is relatively high compared with other γ-ray MSPs (Abdo et al. 2009a). A small fraction of this power would suffice to generate detectable γ-rays from PSR J1023+0038. Given the recent evidence of an accretion disk before 2002 that later disappeared, it is of great importance to probe the energy source that facilitated the dissolution of the disk. The detection of X-rays from the system (Homer et al. 2006) provides a hint that high-energy processes are ongoing, which is further strengthened by the reported X-ray pulsation from PSR J1023+0038 and orbital variability in X-rays (Archibald et al. 2010). These results prompted us to search for γ-rays from the system and to study its X-ray properties in more detail.

2. GAMMA-RAY OBSERVATIONS AND ANALYSIS RESULTS

The Large Area Telescope (LAT) on board the *Fermi Gamma-ray Space Telescope* is able to detect γ-rays with energies between $\sim$20 MeV and $>$300 GeV (Atwood et al. 2009). Data used in this work were obtained between 2008 August 4 and 2010 July 14 that are available at the Fermi Science Support Center.[9] We used the Fermi Science Tools v9r15p2 package to reduce and analyze the data in the vicinity of J1023. Only those data that passed the most stringent photon selection criteria (i.e., the "diffuse" class) were used. To reduce the contamination from Earth albedo γ-rays, we excluded events

---

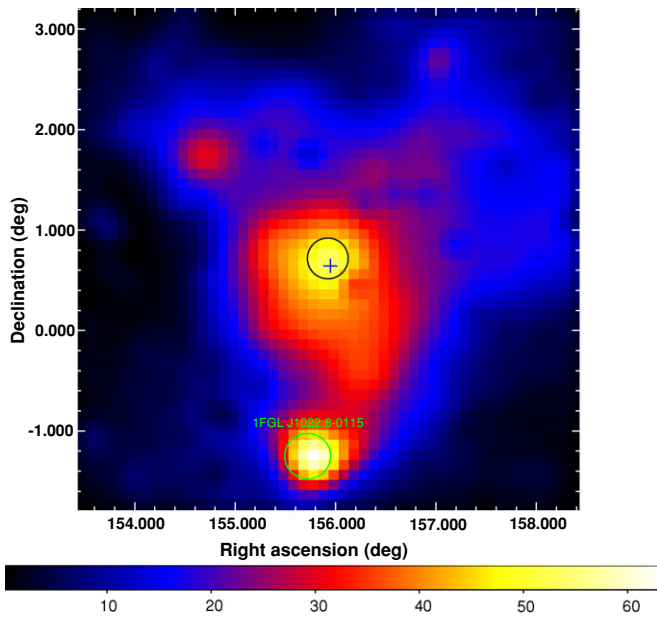**Figure 1.** Test-statistic (TS) map of a region of $5° \times 5°$ centered at the position of J1023 (labeled by the cross). Gamma rays with energies between 200 MeV and 20 GeV were used. This map is created by moving a putative point source through a grid of locations on the sky and maximizing $-\log(\text{likelihood})$ at each grid point, while stronger and well-identified sources outside the sky map are included in each fit. The *Fermi* source 1FGL J1022.8−0115 is clearly seen in the map. The 95% confidence-level error circles of the best-fit position of the γ-ray emission are also shown. The error circle of 1FGL J1022.8−0115 is taken from Abdo et al. (2010b).

with zenith angles greater than $105°$. The instrument response functions "P6_V3_DIFFUSE" recommended for analysis of the "diffuse" class events were used. We chose 200 MeV as the lower energy cut to include sufficient source photons at low energies while reducing the contamination of background photons that dominates at low energies. Therefore, we used events with energies between 200 MeV and 20 GeV in the likelihood analysis.

We carried out an unbinned maximum-likelihood spectral analysis (*gtlike*) of the circular region of $15°$ radius centered on the γ-ray position (see below). We subtracted the background contribution by including the Galactic diffuse model (gll_iem_v02.fit) and the isotropic background (isotropic_iem_v02.txt), as well as all sources in the first *Fermi*/LAT catalog (1FGL; Abdo et al. 2010b) within the circular region of $25°$ radius around the γ-ray position. We assumed a power-law (PL) spectrum for all the 52 1FGL sources considered. The spectral parameter values were set free for sources within $10°$ from J1023.

The maximized test-statistic (TS) value (Mattox et al. 1996) we obtained for the pulsar position is 50, corresponding to a detection significance of 7σ. The position of the γ-ray source is estimated by *gtfindsrc* to be at R.A. (J2000) = $155°.92$ and decl. (J2000) = $0°.72$ with statistical uncertainty $0°.08$ ($0°.2$) at the 68% (95%) confidence level, which is consistent with the position of J1023. The systematic uncertainty is estimated to be $\leqslant 40\%$ (Abdo et al. 2009b). We used *gttsmap* to obtain the TS map of the $5° \times 5°$ region centered on the best-fit γ-ray position, as shown in Figure 1.

To investigate why this γ-ray source was not present in the 1FGL catalog, we divided the whole data set into two: the first and second year data, respectively, and performed the likelihood analysis for each of them separately. Both TS values drop to

22–24, which are about half of the TS value derived using the whole data set and below the threshold of TS = 25 to be included in the 1FGL catalog (Abdo et al. 2010b). This suggests that the source we found is significant (i.e., $>5\sigma$) with two-year data. The spectral parameters from each data set are also consistent with the values reported below.

We then fit the γ-ray spectrum with a single PL, resulting in a photon index of 2.9 ± 0.2 and an integrated energy flux above 200 MeV of $(5.5 \pm 0.9) \times 10^{-12}$ erg cm^{-2} s^{-1}. We divided the 200 MeV–20 GeV γ-rays into five energy bins of logarithmically equal bandwidths and reconstructed the flux using *gtlike* for each band separately, assuming a PL model with $\Gamma_\gamma = 2.9$ within each bin. No γ-ray source was needed at the J1023 position in the three bins above 1.3 GeV (derived TS values <5) in the likelihood analysis, indicating a cutoff at ~ 1 GeV. We therefore attempted to fit the 200 MeV–20 GeV spectrum with a PL with an exponential cutoff (PLE). We found that PLE also well describes the spectrum, i.e., both PL and PLE models gave the same TS value of 50. However, it should be noted that a spectral cutoff is statistically not required. Due to the low photon statistics (~ 280 modeled photons from J1023), the spectral parameters of the PLE model cannot be well constrained simultaneously. Motivated by the possible magnetospheric origin of the γ-rays, Γ_γ and E_c are estimated by fixing the other one (at its mean value) to be 1.9 ± 0.3 and 700 ± 220 MeV. We fixed Γ_γ at 1.5–2.4 (with steps of 0.1) while letting the normalization and E_c free, and found that E_c was only well constrained when $\Gamma_\gamma = 1.7$–2.1, consistent with the above result.

At the distance of 1.3 kpc, the γ-ray luminosity (above 200 MeV) is $(1.1 \pm 0.2) \times 10^{33}$ erg s^{-1}. Assuming that the γ-rays come from PSR J1023+0038 (see Section 3), the pulsar spin-down luminosity $\dot{E} < 3 \times 10^{35}$ erg s^{-1} (Archibald et al. 2009) implies a γ-ray conversion efficiency of only $\gtrsim 0.3\%$. Such γ-ray luminosity and γ-ray efficiency are among the smallest of γ-ray MSPs. Moreover, assuming that the PLE model is robust, the cutoff energy of ~ 700 MeV is the lowest among all γ-ray MSPs. The spectral properties of the γ-ray emission from J1023 are summarized in Table 1.

A search for pulsation of the >10 MeV γ-rays within a $1°$ radius region around the γ-ray position was performed. We did not find any significant pulsed detection at or close to the spin period of the pulsar nor any indication of γ-ray variability related to the orbital modulation. Even so, given the low photon statistics (of just over 700 photons), this result does not preclude any γ-ray pulsation.

We also performed a long-term temporal analysis of J1023 in which the two-year data were binned in three-month periods. No significant γ-ray variability was found, indicating that the object is stable (down to three-month periods) in radiating γ-rays.

3. A MODEL OF γ-RAY EMISSION FROM PSR J1023+0038

The γ-rays from J1023 originate either from the pulsar magnetosphere or a shock where material overflowing from the companion interacts with the pulsar wind. In the pulsar wind scenario, γ-rays may be generated as synchrotron radiation of the electrons and positrons accelerated in the shock (Takata & Taam 2009). An important theoretical uncertainty is how a particle kinetic-dominated flow can be formed near the pulsar (Kirk & Skjæraasen 2003; Arons 2008). In addition, it is also difficult to explain the steep PL spectrum ($\Gamma_\gamma \sim 3$) in the synchrotron

Table 1
Spectral Parameter Values of γ-ray Emission from J1023

Model[a]	Photon Flux[b] (>200 MeV) (10^{-9} cm^{-2} s^{-1})	Energy Flux (>200 MeV) (10^{-12} erg cm^{-2} s^{-1})	Photon Index Γ_γ	Cutoff Energy (MeV)	γ-ray Luminosity[c] (>200 MeV) (10^{33} erg s^{-1})
PL	8.2 ± 1.6	5.5 ± 0.9	2.9 ± 0.2	—	1.11 ± 0.18
PLE	8.1 ± 1.5	5.2 ± 0.8	1.9[d]	700 ± 230	1.06 ± 0.17
PLE	7.8 ± 1.5	5.1 ± 0.8	1.9 ± 0.3	700	1.03 ± 0.17

Notes.
[a] PL: power-law model; PLE: power law with an exponential cutoff model.
[b] All the quoted errors are statistical and 1σ for one parameter of interest.
[c] The pulsar distance is taken as 1.3 kpc.
[d] Model parameters without quoted errors are fixed at the value given.

model. On the other hand, if the pulsar magnetosphere is sufficiently clear of matter, GeV γ-ray photons can be produced in a slot-gap (Harding et al. 2005) or an outer-gap accelerator (Cheng et al. 1986a, 1986b). The curvature radiation from a gap accelerator is expected to have a PLE shape. The reported X-ray pulses from PSR J1023+0038 (Archibald et al. 2010) suggest that the observed γ-rays are also produced in the pulsar magnetosphere. More accumulated source photons in the future should help to answer whether there exists γ-ray pulsation or variability on the timescale of the orbital period, in turn helping to distinguish these two scenarios for the observed γ-rays.

Applying the outer gap model, the γ-ray luminosity is approximately described by

$$L_\gamma \sim f^3 L_{\rm sd}, \qquad (1)$$

where f is the fractional gap thickness, i.e., the ratio of the gap thickness to the radius of the light cylinder, and $L_{\rm sd} = 4(2\pi)^4 B^2 R^6/6c^3 P^4$ is the pulsar spin-down power with B corresponding to the surface magnetic field, R is the stellar radius, and P is the rotation period. The fractional gap thickness is determined by the pair-creation condition between γ-rays emitted in the outer gap and X-rays from the NS surface, i.e., $E_\gamma E_{s,X} = (m_e c^2)^2$, where $E_\gamma \sim 1$ GeV and $E_{s,X}$ are the typical energy of the γ-rays and the X-rays, respectively. Assuming $E_{s,X} = 30$ eV (see Section 4 and Table 2), and following Takata et al. (2010b) we find $f \sim 0.5$. The γ-ray luminosity is estimated as $L_\gamma \sim 4 \times 10^{34}$ erg s^{-1} using $L_{\rm sd} = 3 \times 10^{35}$ erg s^{-1}, consistent with the required luminosity from an irradiating source to explain the heating of the companion star (Thorstensen & Armstrong 2005).

We may estimate the γ-ray flux measured on the Earth as $F_\gamma \sim L_\gamma/\delta\Omega d^2 \sim 10^{-9}$ erg cm^{-2} s^{-1}, where $L_\gamma = 3 \times 10^{34}$ erg s^{-1}, the solid angle $\delta\Omega = 2$, and the distance $d = 1.3$ kpc are assumed. This flux is higher than the observed $F_\gamma \sim 5 \times 10^{-12}$ erg cm^{-2} s^{-1}. We note, however, that the γ-ray flux depends on the viewing geometry, because the intensity varies over the γ-ray beam. We carried out a simple three-dimensional calculation using curvature radiation in the outer gap model (cf. Wang et al. 2010; Takata et al. 2007) and found that F_γ increases from $\sim 5 \times 10^{-13}$ erg cm^{-2} s^{-1} to $\sim 10^{-11}$ erg cm^{-2} s^{-1} when the viewing angle, i.e., the angle between the rotational axis of the pulsar and the line of sight, ξ, increases from $\sim 34°$ to $\sim 53°$ (see Archibald et al. 2009), well consistent with the observed γ-ray flux.

4. RE-ANALYSIS OF THE X-RAY DATA

XMM-Newton observations of J1023 were conveyed on 2004 May 12 (hereafter we refer this observation as XMM1) with all

the EPIC cameras operated in full-frame mode and on 2008 November 26 (hereafter XMM2) with the MOS 1/2 CCDs operated in full-frame mode and the PN camera operated in timing mode with a resolution of 0.03 ms.

Archibald et al. (2010) reported an X-ray analysis of J1023, finding a possible X-ray pulsation from PSR J1023+0038 and modulation on the orbital period of the binary. They interpreted the latter as coming from an intrabinary shock and suggested a composite spectral model with a PL plus a possible thermal component. Although this model results in an acceptable goodness of fit, we found that their analysis is apparently incomplete. The X-ray spectrum from the pulsar magnetosphere is typically different from the shock emission (cf. Hui & Becker 2006, 2007, 2008), and the combined contribution from the two emission regions cannot be generally described by a single PL. To complement their results, we report our independent analysis of these *XMM-Newton* observations.

As PN data obtained from XMM2 are collapsed into a one-dimensional row, they are not suitable for spectroscopy. After filtering for the high sky background and events affected by bad pixels, the effective exposures are 14.9 (MOS 1/2) and 11.6 ks (PN) for XMM1, and 33.5 ks (MOS1/2) for XMM2.

To avoid contamination from a nearby X-ray source, we extracted the energy spectrum of J1023 from the circles with radius $25''$[10] centered on the radio timing position in all data sets, which corresponds to an encircled energy fraction $\sim 80\%$. The background spectra were sampled from nearby low-count circular regions of radius $40''$ in the corresponding cameras. We grouped each spectrum dynamically to obtain the same signal-to-noise ratio in each data set.

First, we fit the XMM1 and XMM2 data separately with various single-component models. Only the PL model provides a good description of the data in both XMM1[11] and XMM2 (see Table 2). With no indication of spectral and flux variability between data taken in XMM1 and XMM2, we combined both data sets for a constraining spectral analysis.

We found that the single PL model provides an acceptable description of the combined data with the spectral parameters as in Archibald et al. (2010). However, we found systematic deviations in this model, indicating that additional component(s) might be required. Motivated by the possible presence of both pulsed emission and emission dependent on the orbital phase of the binary, we fit the spectrum with a broken power law (BKPL). The goodness of fit was found to be improved significantly

---

[10] Circles of radius $35''$ were used in Archibald et al. (2010) that probably contain a larger amount of contamination from the point-spread function wing of that nearby X-ray source.
[11] Our results for XMM1 are consistent with those reported by Homer et al. (2006).

Table 2
Spectral Parameter Values of X-ray Emission from J1023

Model[a]	Epoch	n_H[b] (10^{20} cm^{-2})	Photon Index[c] Γ_X	E_b/kT (keV)	Unabsorbed Flux[d] (10^{-13} erg cm^{-2} s^{-1})	χ^2_ν (dof)
PL	2004 May 12 (XMM1)	<1.2	$1.30^{+0.04}_{-0.05}$	.../...	$4.6^{+0.5}_{-0.3}$	0.94 (40)
PL	2008 Nov 26 (XMM2)	<0.4	1.29 ± 0.04	.../...	$4.9^{+0.4}_{-0.3}$	1.17 (35)
PL	XMM1 and XMM2	<0.6	1.29 ± 0.03	.../...	$4.7^{+0.3}_{-0.2}$	1.00 (77)
BKPL	XMM1 and XMM2	4.4 ± 1.6	$1.75^{+0.16}_{-0.11}(E < E_b)/1.07^{+0.07}_{-0.06}(E > E_b)$	$1.84^{+0.22}_{-0.16}/...$	$6.3^{+1.6}_{-0.9}$	0.75 (75)
BKPL and NMHA	XMM1 and XMM2	$4.7^{+3.3}_{-1.9}$	$1.76^{+0.17}_{-0.14}(E < E_b)/1.07^{+0.07}_{-0.08}(E > E_b)$	$1.84^{+0.14}_{-0.15}/ < 0.033$	$6.4^{+1.8}_{-0.9}$ (BKPL) < 0.73 (NMHA)	0.76 (74)

Notes.

[a] PL: power-law model; BKPL: broken power-law model; NMHA: non-magnetic hydrogen atmospheric model.

[b] Column absorption.

[c] All quoted errors are 1σ for one parameter of interest.

[d] In the 0.01–10 keV range.

($\chi^2_\nu = 0.75$ for 75 dof.) and no systematic fitting residuals were found (see Figure 2), in contrast with the best-fit model (i.e., single PL model) presented in Figure 1 of Archibald et al. (2010). To statistically address the improvement for the spectral fits from the single PL to the broken PL, we used an *F*-test and found that the *p*-value is 7.7×10^{-6}. Therefore, the additional parameters are required statistically. This behavior was found in both epochs (XMM1 as well as XMM2). The break energy was found to be $E_b = 1.84^{+0.22}_{-0.16}$ keV. The spectrum was found to be steeper (i.e., $\Gamma^1_X = 1.75^{+0.16}_{-0.11}$) at $E < E_b$ than that in the hard band (i.e., $\Gamma^2_X = 1.07^{+0.07}_{-0.06}$). The unabsorbed flux was found to be $f_X = 6.3^{+1.6}_{-0.9} \times 10^{-13}$ erg cm^{-2} s^{-1} (0.01–10 keV). At a distance of $d \sim 1$ kpc, the isotropic X-ray luminosity is $L_X = 7.5^{+1.9}_{-1.1} \times 10^{31}$ erg s^{-1} (0.01–10 keV), corresponding to an X-ray conversion efficiency of $\gtrsim 0.03\%$ of the spin-down luminosity.

As thermal X-rays from the NS surface may also contribute, we estimated the thermal contribution besides the non-magnetic hydrogen atmospheric (NMHA) model with the mass and radius of the NS fixed at $M_{NS} = 1.4 M_\odot$ and $R_{NS} = 10$ km. Nevertheless, this additional thermal model was only required at a confidence level of <50%. Furthermore, with normalization as a free parameter, an unreasonably small source distance of ∼30 pc was inferred. To constrain the possible thermal contribution from the stellar surface, we fixed the normalization corresponding to 1 kpc. This results in the 1σ upper limits of the temperature and the thermal flux contribution to be $kT < 32.76$ eV and $f_X < 7.3 \times 10^{-14}$ erg cm^{-2} s^{-1} (0.01–10 keV), respectively.

The fact that more than one PL index is required to explain the observed X-ray spectrum strongly suggests an additional X-ray contribution from this system besides the magnetospheric radiation. As possible orbital modulation in X-rays has been identified, the additional non-thermal component may come from the intrabinary shock (Archibald et al. 2010). Furthermore, our spectral analysis suggests that the emission below and above the break energy (∼2 keV) might have different origins. Archibald et al. (2010) reported an X-ray pulsation for photons at 0.25–2.5 keV. Whether the emission above ∼2 keV is pulsed remains unclear.

We performed an energy-resolved analysis of the X-ray flux as a function of orbital phase. According to the resultant break energy, we divided the energy range (0.3–10 keV) suitable for timing analysis into two bands: 0.3–2 keV (soft) and 2–10 keV (hard). We found no significant variability at the orbital period
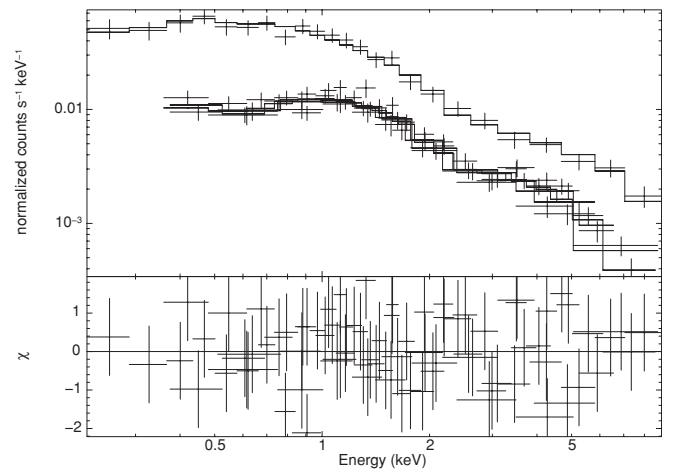

Figure 2. The X-ray spectra of J1023 as obtained from the observations taken at 2004 May 12 and 2008 November 26 with *XMM-Newton* and simultaneously fitted to an absorbed broken power-law model (upper panel) and contribution to the χ^2-fit statistic (lower panel).

in both bands from XMM1 data, consistent with Homer et al. (2006). This is likely due to low photon statistics, as well as insufficient orbital coverage of ∼91% for MOS1/2 and ∼82% for PN data. We therefore focused on the XMM2 data in this study. The orbital light curves of the soft and hard bands are shown in Figure 3. Both soft and hard X-rays contribute to the orbital modulation and the troughs and peaks in the orbital light curves in these two bands occur at the same orbital phases (around 0.2 and 0.6, respectively). Using a χ^2-test, the significance for a flux modulation over the observed orbit in the soft and hard bands was found to be ∼99.1% and ∼85.5%, respectively. Although the significance derived from this test is higher for soft X-rays than for hard X-rays, we could not determine the energy band for which the modulation is greater.

5. CONCLUDING REMARKS

We have found strong evidence for γ-ray emission from an LMXB system, FIRST J102347.67+003841.2. The γ-rays may originate from PSR J1023+0038 or possibly from the intrabinary shock between the pulsar and its companion star. Given the observed steep spectrum ($\Gamma_\gamma \sim 3$), synchrotron emission from the shock is not favored. We have applied an outer gap model to explain the observed γ-rays. Recently, Takata et al. (2010a) suggest that such γ-rays from a newly born MSP may be
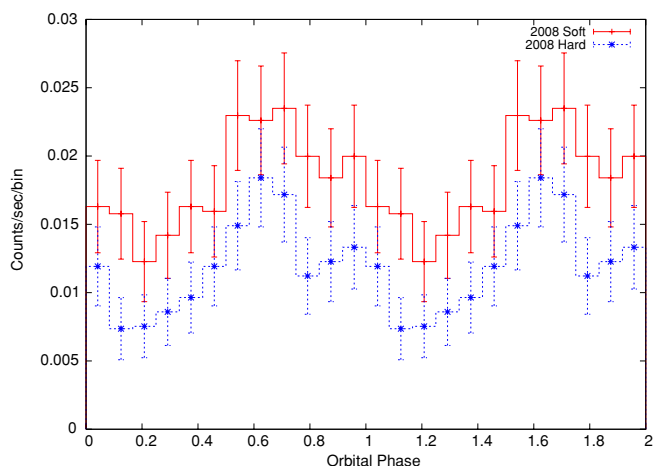
Figure 3. Energy-resolved X-ray light curves of J1023 in the soft (0.3–2.0 keV) and hard (2.0–10.0 keV) bands, as obtained from the observation taken at 2008 November 26 with *XMM-Newton*.

responsible for the disk clearance in such systems. Our discovery of γ-rays, once confirmed, from FIRST J102347.67+003841.2 conform with their predictions.

The spectral analysis of the *XMM-Newton* data taken in 2004 and 2008 suggests that a broken PL well describes the X-ray data, with the lowest systematics, compared to a single PL and other composite models tested. Our X-ray spectral analysis suggests that there exists two components and that both components appear to vary with the orbital phase, supporting the X-ray variability study by Archibald et al. (2010) that suggested more than one mechanism contributes to the observed X-ray flux from J1023.

In such a system that recently transited from the LMXB phase to the radio MSP phase, we speculate that the current state may not be permanent as an accretion disk may reform about the NS in PSR J1023+0038 switching off the radio MSP. A cycle of on and off states of pulsar activity could repeat in the near future. Continuous monitoring in all wavelengths of this unique source will test this idea and help us to comprehend the ongoing evolution of FIRST J102347.67+003841.2.

REFERENCES

Abdo, A. A., et al. (Fermi/LAT Collaboration) 2009a, Science, 325, 848
Abdo, A. A., et al. (Fermi/LAT Collaboration) 2009b, ApJS, 183, 46
Abdo, A. A., et al. (Fermi/LAT Collaboration) 2010a, ApJ, 712, 957
Abdo, A. A., et al. (Fermi/LAT Collaboration) 2010b, ApJS, 188, 405
Alpar, M. A., Cheng, A. F., Ruderman, M. A., & Shaham, J. 1982, Nature, 300, 728
Archibald, A. M., et al. 2009, Science, 324, 1411
Archibald, A. M., et al. 2010, ApJ, 722, 88
Arons, J. 2008, in AIP Conf. Proc. 983, 40 Years of Pulsars: Millisecond Pulsars, Magnetars and More, ed. C. Bassa et al. (Melville, NY: AIP), 200
Atwood, W. B., et al. (Fermi/LAT Collaboration) 2009, ApJ, 697, 1071
Bhattacharya, D., & van den Heuvel, E. P. J. 1991, Phys. Rep., 203, 1
Cheng, K. S., Ho, C., & Ruderman, M. 1986a, ApJ, 300, 500
Cheng, K. S., Ho, C., & Ruderman, M. 1986b, ApJ, 300, 522
Harding, A. K., Usov, V. V., & Muslimov, A. G. 2005, ApJ, 622, 531
Homer, L., et al. 2006, AJ, 131, 562
Hui, C. Y., & Becker, W. 2006, A&A, 448, L13
Hui, C. Y., & Becker, W. 2007, A&A, 470, 965
Hui, C. Y., & Becker, W. 2008, A&A, 486, 485
Kirk, J. G., & Skjæraasen, O. 2003, ApJ, 591, 366
Mattox, J. R., et al. 1996, ApJ, 461, 396
Romanova, M. M., Ustyugova, G. V., Koldoba, A. V., & Lovelace, R. V. E. 2009, MNRAS, 399, 1802
Takata, J., Chang, H.-K., & Cheng, K. S. 2007, ApJ, 656, 1044
Takata, J., Cheng, K. S., & Taam, R. E. 2010a, ApJ, 723, L68
Takata, J., & Taam, R. E. 2009, ApJ, 702, 100
Takata, J., Wang, Y., & Cheng, K. S. 2010b, ApJ, 715, 1318
Thorstensen, J. R., & Armstrong, E. 2005, AJ, 130, 759
Wang, Y., Takata, J., & Cheng, K. S. 2010, ApJ, 720, 178
Wang, Z., Archibald, A. M., Thorstensen, J. R., Kaspi, V. M., Lorimer, D. R., Stairs, I., & Ransom, S. 2009, ApJ, 703, 2017